



Originally published as:

Finger, F., Waitzinger, M., Förster, H.-J., Kozlik, M., Raith, J. (2017): Identification of discrete low-temperature thermal events in polymetamorphic basement rocks using high spatial resolution FE-SEM-EDX U-Th-Pb dating of uraninite microcrystals. - *Geology*, 45, 11, pp. 991—994.

DOI: <http://doi.org/10.1130/G39370.1>

# Identification of discrete low-temperature thermal events in polymetamorphic basement rocks using high spatial resolution FE-SEM-EDX U-Th-Pb dating of uraninite microcrystals

F. Finger<sup>1</sup>, M. Waitzinger<sup>1</sup>, H.J. Förster<sup>2</sup>, M. Kozlik<sup>3</sup>, and J.G. Raith<sup>3</sup>

<sup>1</sup>Department of Chemistry and Physics of Materials, University of Salzburg, Jakob Haringer Straße 2, A-5020 Salzburg, Austria

<sup>2</sup>Helmholtz Zentrum Potsdam Deutsches GeoForschungsZentrum GFZ, Telegrafenberg A 69, 14473 Potsdam, Germany

<sup>3</sup>Department Angewandte Geowissenschaften und Geophysik, Montanuniversität Leoben, Peter-Tunner Straße 5, A-8700 Leoben, Austria

## ABSTRACT

**Low-temperature thermal events of Permian (ca. 265 Ma) and Triassic (ca. 215 Ma) age that predate medium-grade regional metamorphism were identified using high spatial resolution field emission–scanning electron microscopy–energy dispersive X-ray (FE-SEM-EDX) U-Th-Pb dating of uraninite microcrystals in basement rocks of the Tauern Window, Eastern Alps. Three novel points of generic geochronological importance are raised in this study. First, uraninite can be meaningfully dated with FE-SEM-EDX methods, with moderate precision. Second, uraninite is geochronologically robust, even at microcrystal scale, and can survive at least medium-grade metamorphic overprint without being reset. Third, uraninite microcrystals are powerful tools for identifying and dating discrete low-temperature thermal events in orogenic belts. Dating of uraninite microcrystals should be considered an important complementary geochronological method in the study of polymetamorphic rocks.**

## INTRODUCTION

Unravelling the full geological history of basement terranes using geochronological methods is not a simple task, because regional metamorphism may obscure, or even obliterate, older crystallization stages. Precise temporal constraints on, and identification of, thermal events that predate medium-grade regional metamorphism is generally only possible if these early events involved crystallization of robust datable minerals such as zircon, monazite, or garnet. These minerals typically form under higher temperature ( $T$ ) conditions ( $>500$  °C) and less frequently during lower  $T$  events. Thus, low-temperature events that predate medium-grade regional metamorphism can easily remain undetected in geochronological studies, although they may have great significance, for example in understanding ore-forming processes in basement terranes.

Dating of accessory uraninite microcrystals provides a new approach for identifying, and temporally constraining, such low- $T$  thermal events that predate regional metamorphism. The use of microcrystals for geochronology presents a challenge because state of the art in situ dating methods such as sensitive high-resolution ion microprobe (SHRIMP) or laser-based U-Pb isotope dating involve spot-sizes of  $>5$   $\mu\text{m}$ , which do not allow for precise targeting of minute grains. Electron beam analysis offers a much finer spatial resolution ( $\sim 1$   $\mu\text{m}$  at 15 kV), and

may thus be the first choice for the total Pb dating of micron-sized uraninite crystals. Using the Tauern Window of the Eastern Alps as an example, we show that uraninite microcrystals ( $<10$   $\mu\text{m}$ ) are not only widespread in certain types of metamorphic rocks, but are also geochronologically robust, and enable identification and dating of events that predate regional metamorphism in this terrane.

## GEOLOGICAL BACKGROUND

The Tauern Window exposes the deepest tectonic units of the Eastern Alps (Fig. 1A). It contains crustal rocks of the European plate that were overridden by various nappes derived from the southern Adriatic plate during the Alpine orogeny (see Schmid et al., 2004, 2013, for review). As a consequence of this tectonic burial, the Tauern Window underwent upper greenschist to middle amphibolite facies regional metamorphism in the late Paleogene. Regional metamorphism has been well constrained by various geochronological studies, including K-Ar, Ar-Ar, and Rb-Sr mica and hornblende dating, and Sm-Nd garnet dating (data compilation in Pestal et al., 2009). Approximately half of the Tauern Window complex consists of the so-called Penninic units (Fig. 1B) of Mesozoic sedimentary and volcanic rocks, including obducted Jurassic–Cretaceous ophiolites (Frasl and Frank, 1966; Höck, 1983). An older, pre-Mesozoic basement (Subpenninic units in Fig.

1B) of early Paleozoic island arc-type crust was variably metamorphosed during the Variscan period (Habach Complex and Altkristallin; Fig. 1B), and intruded by large volumes of Variscan granitoids, now called the Central Gneisses.

The pre-Alpine geochronology of the Tauern Window is mainly based on Carboniferous to Permian zircon dates from the Variscan granitoids (Eichhorn et al., 2000; Vesela et al., 2012) and Cambrian–Ordovician to Devonian zircon dates from the older arc-type crust (Eichhorn et al., 1995; Kebede et al., 2005). Carboniferous (Variscan) metamorphism is recorded in garnet and monazite ages (von Quadt 1992; Finger et al., 2016).

## ACCESSORY URANINITE CRYSTALS IN ROCKS FROM THE TAUERN WINDOW

Microcrystals (1–10  $\mu\text{m}$ ) of accessory uraninite were identified during petrographic, scanning electron microscopy (SEM), and energy dispersive X-ray (EDX) reinvestigation of Variscan metagranitoids from the central Tauern Window, including the K1 gneiss of the Felbertal scheelite mine, the Felbertauern augengneiss, the Granatspitz granite gneiss, and the Reichen-spitz aplite gneiss (Fig. 1B). Petrographic information is provided in the GSA Data Repository<sup>1</sup>. Zircon dating (Eichhorn et al., 2000; Kozlik et al., 2016) defines the first two rocks as early Carboniferous granites ( $339.6 \pm 1.2$  Ma,  $338.5 \pm 1.3$  Ma), whereas the Granatspitz and Reichen-spitz gneisses are younger Permian intrusions ( $271 \pm 4$  Ma,  $292 \pm 6$  Ma).

On average, 10–20 uraninite microcrystals were observed in a single thin section. Many are enclosed within zircon (Fig. 2A). Some are included in feldspars, epidote, or titanite

<sup>1</sup>GSA Data Repository item 2017335, sample descriptions, whole-rock geochemistry data and representative SEM-EDX uraninite analyses, and Tables DR1–DR3, is available online at <http://www.geosociety.org/datarepository/2017/> or on request from [editing@geosociety.org](mailto:editing@geosociety.org).

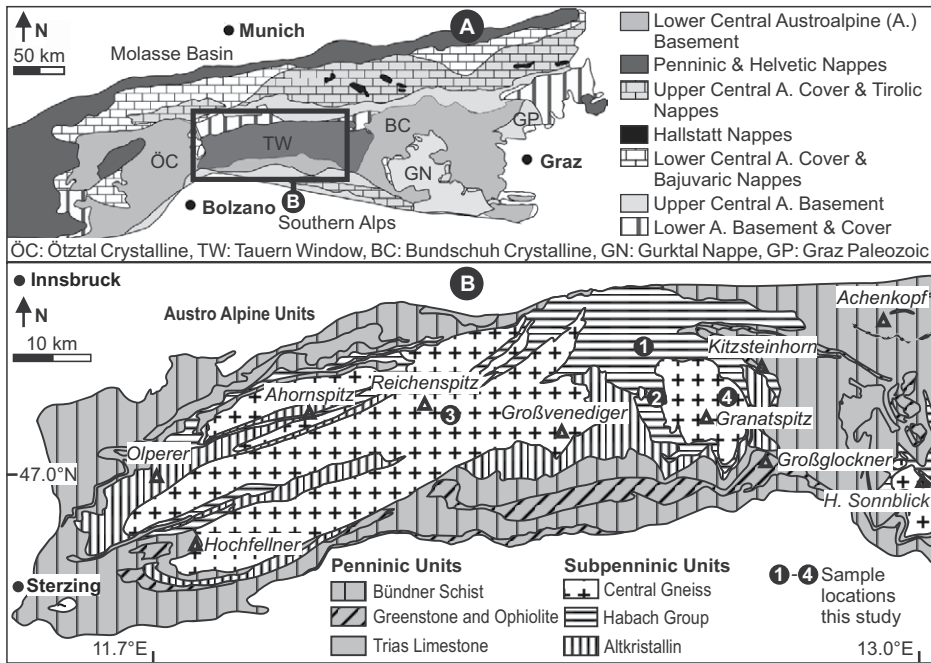


**Figure 1. A:** Tectonic overview map of the Eastern Alps (after Schmid et al., 2013). **B:** Geological map of the Tauern Window (after Pestal et al., 2009), showing sample locations.

(Fig. 2B). Swarms of uraninite microcrystals are present in some quartz-chlorite veins (Fig. 2C). Most uraninite crystals display a uniform gray-scale in backscattered electron (BSE) images, implying compositional homogeneity. However, a few grains exhibit a weak internal zonation with a slightly brighter rim, or irregular and diffuse patchy zonation (Figs. 2D and 2E).

#### ANALYTICAL PROCEDURE

Uraninite microcrystals were analyzed with a Zeiss Ultraplus SEM equipped with a field emission cathode (FE-SEM) and an EDX large-area silicon-drift detector (Oxford X-Max50). An analytical precision of  $\sim 0.9$  and  $0.1$  wt% ( $1\sigma$ ) was achieved for U ( $M\alpha$ ) and Pb ( $M\alpha$ ), respectively, using an accelerating voltage of 15 kV

(2 nA beam current,  $\sim 200$  nm beam width) and a counting time of 3–5 min per spot. This analytical uncertainty corresponds to an age error of  $\sim 20$  m.y. ( $1\sigma$ ). Quantification of concentrations is based on intensity values taken from the Oxford Instruments INCA Energy internal standard data bank and a 180 s calibration measurement on copper before every analytical session. Background, line interference, and matrix corrections are automatically carried out by the INCA Energy software.

A Pb-free synthetic  $UO_2$  crystal was measured to control the Pb background, which is one of the most critical parameters for U–Th–total Pb dating (Williams and Jercinovic, 2002). A small but systematic blank value of  $-0.16 \pm 0.06$  wt% PbO was recognized and externally corrected based on the assumption that it was constant during every uraninite analysis. The uncertainty of the blank value was incorporated in the total Pb error and the age error. The accuracy of the dating procedure was monitored by two in-house uraninite age standards: hydrothermal uraninite from Mitterberg, Austria, previously dated as  $90 \pm 5$  Ma (Paar and Köppl, 1978), and uraninite-bearing granite from the Erzgebirge, Germany, dated as  $326 \pm 4$  Ma (Förster, 1999) and  $330 \pm 5$  Ma (Kempe, 2003).

At 15 kV, the electron beam excitation volume in uraninite is slightly  $< 1$   $\mu$ m in diameter (Drouin et al., 2007). Therefore, a large number of spot analyses (6–15) can be placed within a single crystal; this allows identification of any compositional heterogeneity. Analyses were commonly carried out along rim-core-rim

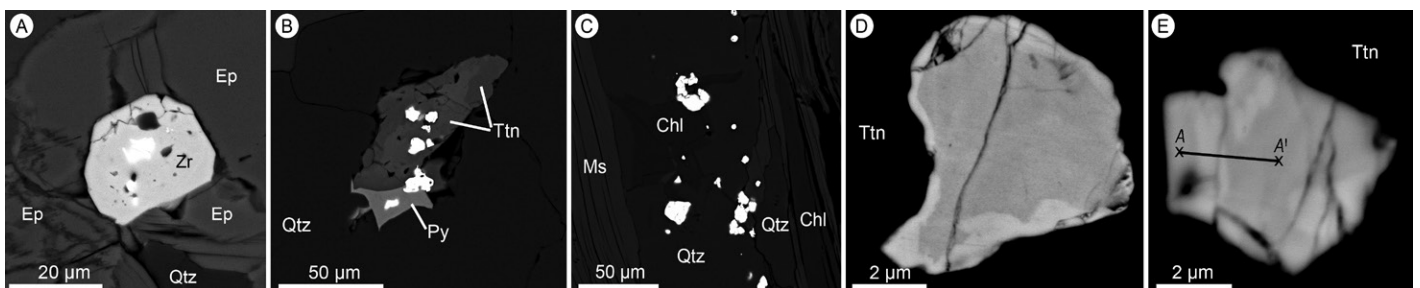


**Figure 2. Backscattered electron images of uraninite microcrystals (brightest grains). Chl—chlorite; Ep—epidote; Ms—muscovite; Py—pyrite; Ttn—titanite; Qtz—quartz; Zr—zircon (mineral abbreviations are after Kretz, 1983). A, B:** Uraninite inclusions in zircon and titanite (K1 gneiss). **C:** Uraninite crystals in chlorite quartz vein (Granatspitz gneiss). **D, E:** Patchily zoned polygenetic uraninite (Granatspitz gneiss and Felbertauern augengneiss; profile A-A' refers to Fig. 3E).

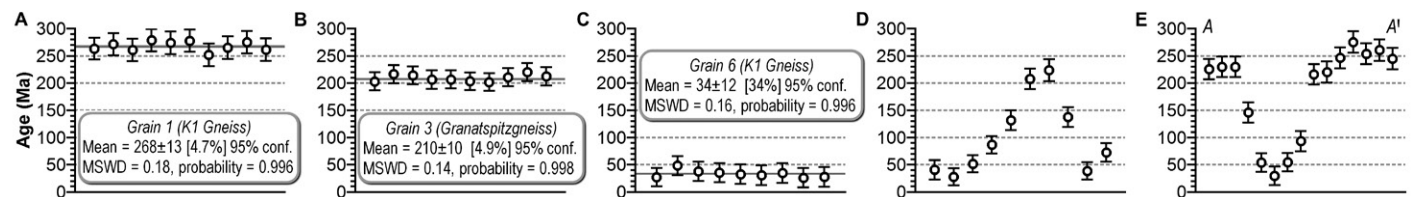


**Figure 3. High spatial resolution chemical age profiles (step width 200–500  $\mu$ m) across single uraninite microcrystals. A–C:** Homogeneous age distribution examples with calculated single grain ages of  $268 \pm 13$ ,  $210 \pm 10$ , and  $34 \pm 12$  Ma, respectively. MSWD—mean square of weighted deviates; conf.—confidence. **D, E:** Polygenetic uraninite grains with heterogeneous age distributions (Granatspitz gneiss and Felbertauern augengneiss).

profiles using a step width of  $\sim 0.5 \mu\text{m}$  (Fig. 3). Crystals, which showed heterogeneities in BSE imaging, were measured with traverses perpendicular to their compositional zonation.

In approximately two-thirds of the targeted uraninite crystals, individual spot ages were uniform within error and were statistically averaged to produce a single grain age, with errors typically between 10 and 20 m.y. (95% confidence level), depending on the number of points analyzed. Mean ages were not calculated for those uraninites that yielded significant internal age scatter. Such grains are considered to be polygenetic or chemically altered.

## RESULTS

### Single Grain Uraninite Ages

Uraninite crystals with a consistent internal age distribution (e.g., Figs. 3A–3C) define three different age groups: (1) those with Permian ages (ca. 265 Ma) from the two Carboniferous granitoids (K1 gneiss and Felbertauern augengneiss), (2) those with ages of ca. 215 Ma from the Permian granitoids (Granatspitz and Reichenspitz gneisses), and (3) those with ages of ca. 30 Ma from the K1 gneiss, the Felbertauern augengneiss, and the Granatspitz gneiss. The results are shown graphically in Figure 4, together with the ages obtained for the standards. Representative analyses are listed in Table DR2 in the Data Repository. In addition to U and Pb, minor amounts of Th (0.4–9 wt%), Y (<5 wt%), and traces of Ca and heavy rare earth elements were measured in most grains.

### Polygenetic Uraninite Crystals

In some grains, Pb contents (and ages) strongly decrease from core to rim (Fig. 3D), whereas in other cases, significantly younger ages are recorded in the interior parts of the crystals (Fig. 3E), associated with bright patchy zonation observed in the BSE images (Fig. 2E). Constant age plateaus are rarely observed in these polygenetic grains, and thus the geochronological dates were deemed uninterpretable. However, given the fact that the oldest measured ages (ca. 270 and 210 Ma) overlap the two oldest single grain age groups (ca. 265 Ma and ca. 215 Ma), and the youngest ages are indistinguishable from the third single grain age group (ca. 30 Ma; Fig. 4), the data are consistent with an interpretation that Permian and Triassic uraninite crystals were compositionally altered by fluid-induced dissolution-reprecipitation mechanisms during later Alpine orogenesis in the Paleogene.

## DISCUSSION AND CONCLUSIONS

### Interpretation of the Uraninite Ages and Regional Geologic Implications

Attempts to assess the crystallization age of any U-rich mineral based on total Pb concentrations

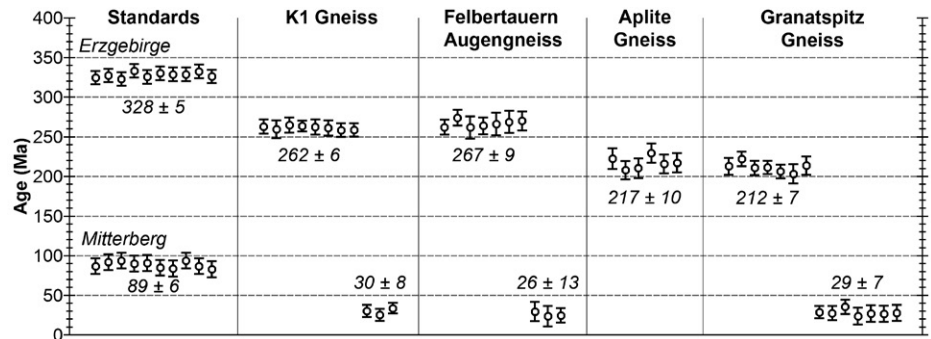


**Figure 4.** Single grain ages of 51 uraninite crystals from the 4 rocks studied and data for the 2 standards. Individual errors are  $1\sigma$ , average ages are at 95% confidence level.

must take into account the potential influence of the initial lead contents, as well as the possibility that the U–Th–Pb system did not remain closed. Initial Pb contents in uraninite are, in general, negligibly low (Fayek et al., 2002), but the risk of determining ages that reflect a post-crystalline disturbance of the U–Th–Pb system should not be underestimated. Pb loss, as well as U loss or gain, can occur during any fluid-driven post-crystallization alteration event (Kempe, 2003; Alexandre and Kyser, 2005; Chipley et al., 2007; Pal and Rhede, 2013). However, if a uniform age is reproduced across a single crystal, it is argued that the U–Th–Pb concentrations remained undisturbed, and valid age information can be obtained. Clearly, if identical intercrystal chemical ages are reproduced across several grains, the geological significance of the age is increased.

With this criterion in mind, we consider the 3 uraninite age groups of ca. 265 Ma, ca. 215 Ma, and ca. 30 Ma as geologically meaningful, particularly because they can be linked to distinct geological events in the evolution of the Tauern Window. The ca. 30 Ma uraninite ages coincide with Paleogene regional metamorphism associated with the Alpine orogeny (Pestal et al., 2009). The 2 uraninite age groups of ca. 265 and ca. 215 Ma predate the Alpine regional metamorphism, but are significantly younger than the zircon ages of their granitoid host. Thus, the ca. 265 and ca. 215 Ma dates cannot be interpreted as magmatic ages and likely record discrete hydrothermal or low-grade metamorphic events. There is unequivocal evidence for ca. 270 Ma granitic activity in the Tauern Window from zircon dating (Eichhorn et al., 2000). It is thus proposed that the ca. 265 Ma uraninite ages in the Carboniferous granitoids record low-grade Permian metamorphism or hydrothermal activity associated with this ca. 270 Ma intrusive event.

Uraninite formation at ca. 215 Ma is geologically meaningful in that Pangea began to break apart during the Triassic. The sedimentary record of the Tauern Window indicates normal-fault bound, deep basin conditions at that time (Pestal et al., 2009). Thus, the Subpenninic units

of the Tauern Window, and adjacent areas within the European plate, were likely exposed to an increased heat and fluid flow during the Triassic.

Future studies must attempt to constrain the pressure–temperature conditions for these two Permian–Triassic events recorded in the U–Th–total Pb ages of the uraninite microcrystals. The degree of crustal heating was probably low grade in both periods, and most of the low-*T* minerals that were produced at that time were obliterated by the penetrative Paleogene regional metamorphism. Notably, metamorphic or hydrothermal minerals from the Permian–Triassic Periods have very rarely been reported in the Tauern Window, despite the numerous multimethod geochronological studies. Here, uraninite dating may provide a completely new and powerful approach.

### Methodical Aspects Regarding the Use of Uraninite as a Geochronometer

The successful application of in situ U–Th–total Pb dating of uraninite by means of electron beam excitation and X-ray spectroscopy dates to before the more popular U–Th–total Pb dating of monazite (Parslow et al., 1985; Bowles, 1990), but the method has never been widely used. It has been restricted to studies of uraninite in uranium deposits (Alexandre and Kyser, 2005; Cross et al., 2011; Pal and Rhede, 2013) and to accessory magmatic uraninite in granitic rocks (Förster, 1999; Kempe, 2003; Cocherie and Legendre, 2007; Förster et al., 2012).

Here we show for the first time that U–Th–total Pb dating can be successfully applied to uraninite microcrystals in metamorphic rocks. The potential application of uraninite dating in metamorphic terranes relies on the fact that uraninite is geochronologically robust. We demonstrate that even very small uraninite crystals can survive an amphibolite facies overprint without their U–Th–Pb systematics being significantly disturbed or reset. Many crystals that we measured during this study did not show Pb loss despite having been subjected to temperatures of  $\sim 500$ – $550^\circ\text{C}$  during a much younger, penetrative regional metamorphic event. However,

note that chemical alteration of older uraninite grains was observed and can take place during metamorphism, most probably via dissolution-precipitation. For a successful dating of uraninite in metamorphic rocks, it is imperative to record internal textures and high-resolution compositional profiles across single crystals.

We briefly comment on the potential of the field emission-scanning electron microscopy-energy dispersive X-ray method for U-Th-total Pb uraninite dating. We propose that the special construction, particularly the high beam stability, of modern FE-SEMs is advantageous for high spatial resolution measurements, as is the ability of EDX detectors to analyze all elements simultaneously. We are aware that quantitative EDX spectral analysis is viewed by many with skepticism, and considered inferior compared to wavelength dispersive analysis (WDX). However, in our study the EDX results have proved reproducible in several control measurements using WDX microprobe analysis (see the Data Repository). Furthermore, repeated analyses of two in-house uraninite age standards have confirmed the validity of the calculated dates (Fig. 4). In conclusion, we assume that state of the art FE-SEM-EDX techniques (with large-area silicon-drift detectors) provide sufficient accuracy for uraninite dating owing to the circumstance that radiogenic Pb is abundant in uraninite.

#### ACKNOWLEDGMENTS

The study received support through the Austrian Science Fund project P 22480 (to Finger). We thank Charles A. Geiger and Noreen Vielreicher for style and linguistic improvements of the text, and C. Hetherington, M. Williams, and an anonymous reviewer for helpful comments.

#### REFERENCES CITED

- Alexandre, P., and Kyser, T.K., 2005, Effects of cationic substitutions and alteration in uraninite, and implications for the dating of uranium deposits: *Canadian Mineralogist*, v. 43, p. 1005–1017, doi:10.2113/gscanmin.43.3.1005.
- Bowles, J.F.W., 1990, Age dating of individual grains of uraninite in rocks from electron microprobe analyses: *Chemical Geology*, v. 83, p. 47–53, doi:10.1016/0009-2541(90)90139-X.
- Chipley, D., Polito, P.A., and Kyser, T.K., 2007, Measurement of U-Pb ages of uraninite and davidite by laser ablation-HR-ICP-MS: *American Mineralogist*, v. 92, p. 1925–1935, doi:10.2138/am.2007.2226.
- Cocherie, A., and Legendre, O., 2007, Potential minerals for determining U-Th-Pb chemical age using electron microprobe: *Lithos*, v. 93, p. 288–309, doi:10.1016/j.lithos.2006.03.069.
- Cross, A., Jaireth, S., Rapp, R., and Armstrong, R., 2011, Reconnaissance-style EPMA chemical U-Th-Pb dating of uraninite: *Australian Journal of Earth Sciences*, v. 58, p. 675–683, doi:10.1080/08120099.2011.598190.
- Drouin, D., Couture, A.R., Joly, D., Tastet, X., Aimez, V., and Gauvin, R., 2007, CASINO V2.42—A fast and easy-to-use modeling tool for scanning electron microscopy and microanalysis users: *Scanning*, v. 29, p. 92–101, doi:10.1002/sca.20000.
- Eichhorn, R., Schärer, U., and Höll, R., 1995, Age and evolution of scheelite-hosting rocks in the Felbertal deposit (Eastern Alps): U-Pb geochronology of zircon and titanite: *Contributions to Mineralogy and Petrology*, v. 119, p. 377–386, doi:10.1007/BF00286936.
- Eichhorn, R., Loth, G., Höll, R., Finger, F., Schermaier, A., and Kennedy, A., 2000, Multistage Variscan magmatism in the central Tauern Window (Austria) unveiled by U/Pb SHRIMP zircon data: *Contributions to Mineralogy and Petrology*, v. 139, p. 418–435, doi:10.1007/s004100000145.
- Fayek, M., Kyser, T.K., and Riciputi, L.R., 2002, U and Pb isotope analysis of uranium minerals by ion microprobe and the geochronology of the McArthur River and Sue Zone uranium deposits, Saskatchewan, Canada: *Canadian Mineralogist*, v. 40, p. 1553–1570, doi:10.2113/gscanmin.40.6.1553.
- Finger, F., Krenn, E., Schulz, B., Harlov, D., and Schiller, D., 2016, “Satellite monazites” in polymetamorphic basement rocks of the Alps: Their origin and petrological significance: *American Mineralogist*, v. 101, p. 1094–1103, doi:10.2138/am-2016-5477.
- Förster, H.J., 1999, The chemical composition of uraninite in Variscan granites of the Erzgebirge, Germany: *Mineralogical Magazine*, v. 63, p. 239–252, doi:10.1180/002646199548466.
- Förster, H.-J., Rhede, D., Stein, H., Romer, R.L., and Tischendorf, G., 2012, Paired uraninite and molybdenite dating of the Königshain granite: Implications on the onset of late Variscan magmatism in the Lausitz Block (Germany): *International Journal of Earth Sciences*, v. 101, p. 57–67, doi:10.1007/s00531-010-0631-1.
- Frasl, G., and Frank, W., 1966, Einführung in die Geologie und Petrographie des Penninikums im Tauernfenster mit besonderer Berücksichtigung des Mittelabschnittes im Oberpinzgau, Land Salzburg: *Der Aufschluß Sonderheft*, v. 15, p. 30–58.
- Höck, V., 1983, Mesozoic ophiolites and non-ophiolitic metabasites in the central part of the Tauern Window (Eastern Alps, Austria): *Ofioliti*, v. 8, p. 103–126.
- Kebede, S., Klötzli, U., Kosler, J., and Skiöld, T., 2005, Understanding the pre-Variscan and Variscan basement components of the central Tauern Window, Eastern Alps (Austria): Constraints from single zircon U-Pb geochronology: *International Journal of Earth Sciences*, v. 94, p. 336–353, doi:10.1007/s00531-005-0487-y.
- Kempe, U., 2003, Precise electron microprobe age determination in altered uraninite: Consequences on the intrusion age and the metallogenic significance of the Kirchberg granite (Erzgebirge, Germany): *Contributions to Mineralogy and Petrology*, v. 145, p. 107–118, doi:10.1007/s00410-002-0439-5.
- Kozlik, M., Raith, J.G., and Gerdes, A., 2016, U-Pb, Lu-Hf and trace element characteristics of zircon from the Felbertal scheelite deposit (Austria): New constraints on timing and source of W mineralization: *Chemical Geology*, v. 421, p. 112–126, doi:10.1016/j.chemgeo.2015.11.018.
- Kretz, R., 1983, Symbols for rock-forming minerals: *American Mineralogist*, v. 68, p. 277–279.
- Paar, W., and Köppel, V., 1978, The ‘pitchblende-nodule-assembly’ of Mitterberg (Salzburg, Austria): *Neues Jahrbuch für Mineralogie Abhandlungen*, v. 131, p. 254–271.
- Pal, D.C., and Rhede, D., 2013, Geochemistry and chemical dating of uraninite in the Jaduguda uranium deposit, Singhbhum shear zone, India—Implications for uranium mineralization and geochemical evolution of uraninite: *Economic Geology and the Bulletin of the Society of Economic Geologists*, v. 108, p. 1499–1515, doi:10.2113/econgeo.108.6.1499.
- Parslow, G.R., Brandstätter, F., Kurat, G., and Thomas, D.J., 1985, Chemical ages and mobility of U and Th in anatectites of the Cree Lake Zone, Saskatchewan: *Canadian Mineralogist*, v. 23, p. 543–551.
- Pestal, G., Hejl, E., Braunstingl, R., and Schuster, R., 2009, Erläuterungen Geologische Karte von Salzburg 1:200000: Wien, Geologische Bundesanstalt, 162 p.
- Schmid, S.M., Fügenschuh, B., Kissling, E., and Schuster, R., 2004, Tectonic map and overall architecture of the Alpine orogeny: *Eclogae Geologicae Helvetiae*, v. 97, p. 93–117, doi:10.1007/s00015-004-1113-x.
- Schmid, S.M., Scharf, A., Handy, M.R., and Rosenberg, C.L., 2013, The Tauern Window (Eastern Alps, Austria): A new tectonic map with cross-sections and a tectonometamorphic synthesis: *Swiss Journal of Geoscience*, v. 106, p. 1–32, doi:10.1007/s00015-013-0123-y.
- Vesela, P., Soellner, F., Finger, F., and Gerdes, A., 2012, Magmato-sedimentary Carboniferous to Jurassic evolution of the western Tauern Window, Eastern Alps (constraints from U-Pb zircon dating and geochemistry): *International Journal of Earth Sciences*, v. 100, p. 993–1027, doi:10.1007/s00531-010-0596-0.
- von Quadt, A., 1992, U-Pb zircon and Sm-Nd geochronology of mafic and ultramafic rocks from the central part of the Tauern Window (eastern Alps): *Contributions to Mineralogy and Petrology*, v. 110, p. 57–67, doi:10.1007/BF00310882.
- Williams, M.L., and Jercinovic, M.J., 2002, Microprobe monazite geochronology: Putting absolute time into microstructural analysis: *Journal of Structural Geology*, v. 24, p. 1013–1028, doi:10.1016/S0191-8141(01)00088-8.

Manuscript received 1 June 2017

Revised manuscript received 27 July 2017

Manuscript accepted 27 July 2017

Printed in USA